Microstructure and magneto-optical properties of Pr–Ni substituted Ba hexaferrite films prepared by sputtering

M. Gomi[a)]
Department of Materials Science, Japan Advanced Institute of Science and Technology, Asahidai 1-1, Tatsunokuchi, Ishikawa 923-12, Japan

J. Cho[b)] and M. Abe
Department of Physical Electronics, Tokyo Institute of Technology, Ookayama, Meguro-ku, Tokyo 152, Japan

(Received 4 March 1997; accepted for publication 30 July 1997)

Hexaferrite thin films of $Ba_{1-x}R_xFe_{12-x}Ni_xO_{19}$ (R=Pr, La) were grown on nonmagnetic garnet substrates by rf sputtering. When deposited at a substrate temperature of 550 °C at rf power density (PD_{rf}) larger than 19 W/cm^2, the films were completely crystallized, with the *c* axis preferentially oriented normal to the film plane. Transmission electron microscopy revealed that the films deposited at low PD_{rf} were amorphous but locally contained microcrystallites several nm in size. On the other hand, the films deposited at PD_{rf} larger than 20 W/cm^2 were polycrystalline with a crystallite size as large as 300 nm. Faraday rotation measurements showed that the Ni substitution induced a large negative rotation in the photon energy range of 2.1–2.6 eV. This Ni contribution was predominantly attributed to the crystal-field transition of octahedrally coordinated Ni^{2+} ions lying in the 2 eV range. No contribution by Pr^{3+} ions to the Faraday rotation was observed within the photon energy range measured. © *1997 American Institute of Physics.*
[S0021-8979(97)00822-0]

I. INTRODUCTION

Substitution of specific ions such as Bi^{3+}, Co^{2+}, and light rare earth ions into garnet and spinel ferrites significantly enhances magneto-optical (MO) activity.[1–6] This enhancement is strongly affected not only by the valence state of the enhancement ion but also by the crystallographic environment surrounding the enhancement ion. In fact, it is well known that octahedrally coordinated Co^{2+} in spinel ferrites exhibits little MO enhancement compared with tetrahedrally coordinated Co^{2+}.[5,6] Hexagonal ferrites with the magnetoplumbite (M-type) crystal structure contain both alkaline earth ions and transition metal ions, part of which permits replacements by the above enhancement ions with various ionic radii. Therefore, it is useful to compare the MO activity of the enhancement ions in the hexaferrites with that in rare earth iron garnet in order to clarify the MO behavior of the enhancement ions in different crystallographic sites. Abe and Gomi reported that tetrahedrally coordinated Co^{2+} in hexagonal ferrites gives rise to a large MO effect due to the $^4A_2-^4T_1(P)$ and $^4A_2-^4T_1(F)$ crystal-field transitions around 2.0 and 0.8 eV, respectively.[6] However, with the exception of the above and a recent theoretical study,[7] few studies have been performed on the MO effect of the hexaferrites. This is primarily because the hexaferrite has a complicated crystal structure that makes detailed analysis of the spectrum particularly difficult. In addition, MO measurement requires a specific film with the *c* axis preferentially oriented normal to the film plane in order to avoid birefringence.

In order to examine the contributions of Pr^{3+} and/or Ni^{2+} to the MO effect in the hexagonal structure, we have successfully prepared Pr–Ni substituted M-type Ba hexaferrite (BaM) films with the *c* axis well oriented normal to the film plane by sputtering. The Pr^{3+} ion is known to induce large negative Faraday rotation in the visible region when dodecahedrally coordinated in iron garnet,[3] but the contribution of the Ni^{2+} ion to the MO effect has not yet been determined. In this article, we describe structural and magnetic properties of Pr–Ni substituted BaM films, and discuss the contributions of the substituted ions to Faraday rotation of the films, in comparison with those of the films substituted with La^{3+} instead of Pr^{3+}.

II. EXPERIMENT

The films of $Ba_{1-x}R_xFe_{12-x}Ni_xO_{19}$ (R=Pr, La, $x=0$, 0.3, 0.6) were deposited on $Gd_3Ga_5O_{12}$ (GGG) single crystal substrates at temperatures (T_s) of 400–600 °C using conventional rf diode sputtering. Ceramic disks (70 mm in diameter) were used as targets, the nominal compositions of which are summarized in Table I, along with other sputtering parameters. The trivalent R ions substituted for the Ba^{2+} ions were charge compensated by the same number of divalent Ni ions replaced for the Fe^{3+} ions. Since the resputtering of the Ba element from the film surface by the bombardment of high energy ions during deposition was much greater than that of the other element, it was overdosed in the targets.

The chemical composition of the films was determined by the inductively coupled plasma (ICP) method and by x-ray microanalysis. The crystal structure, surface morphology, and microstructure of the prepared films were evaluated by x-ray diffractometry (XRD), scanning electron microscopy (SEM), and transmission electron microscopy (TEM),

[a)]Electronic mail: gomi@jaist.ac.jp
[b)]Current address: Department of Electronic Materials Engineering, Gyeongsang National University, Gajoa-Dong, Chinju 660-701, Korea.

Downloaded 25 Aug 2010 to 133.68.192.95. Redistribution subject to AIP license or copyright; see http://jap.aip.org/about/rights_and_permissions

TABLE I. Target compositions and sputtering conditions.

Target	$Ba_{1.33(1-x)}R_xFe_{12-x}Ni_{1.5x}O_{19+y}$ (R=Pr, La, $x=0$, 0.3, 0.6)
Sputter gas	Ar:O_2=9:1
Gas pressure	50 mTorr
Incident rf power density	6–24 W/cm^2
Deposition rate	7–20 nm/min
Substrate temperature	400–600 °C

respectively. The Faraday rotation of the films was measured by the polarization modulation method in the photon energy range of 1.5–3 eV.

III. RESULTS AND DISCUSSION

A. Structural and magnetic properties

Typical compositions of the films are compiled in Table II, where the atomic ratio was calculated on the assumption that the amount of Fe per formula unit in the film was equal to that of the target. The film compositions are close to those of the targets, although Ni is slightly richer. It was confirmed that the film composition is nearly independent of the power density (PD_{rf}) of the rf discharge which is a significant parameter that dominates crystallization of the film during deposition.

When $T_s<550$ °C and $PD_{rf}<19$ W/cm^2, the films were x ray amorphous. On the other hand, as the typical XRD spectra of Fig. 1 show, all films deposited at PD_{rf} and/or T_s higher than the above values were fully crystallized in the single phase of M-type hexaferrite with the *c* axis preferentially oriented perpendicular to the film plane. The increase of the substituted amount *x* decreased the film quality, as shown in Fig. 2. This is because the increased *x* induced locally large lattice distortions caused by the difference between the ionic radius of the Ba^{2+} ion and the substituted R^{3+} ion; these distortions resulted in poor crystallinity.

Figure 3 shows typical SEM images of the surface and cross section of $Ba_{1-x}Pr_xFe_{12-x}Ni_xO_{19}$ ($x=0.38$) films deposited at PD_{rf}=9 W/cm^2 [Figs. 3(a) and 3(a′)] and 20 W/cm^2 [Figs. 3(b) and 3(b′)]. The bright field TEM images and selected area diffraction patterns of these films are presented in Fig. 4. The surface of the film deposited at 9 W/cm^2 shows a fine structure, although the film is x ray amorphous. The TEM observation of this film [Figs. 4(a) and 4(a′)] indicated that microcrystallites several nm in size were embedded in the amorphous matrix and caused the broad ring in the diffraction of the selected area. The film deposited at 20 W/cm^2, on the other hand, showed much a greater surface structure. The surface roughness was somewhat smaller

TABLE II. Typical compositions per formula unit of films sputtered at PD_{rf}=20 W/cm^2 and T_s=550 °C, where it was assumed that the amount of Fe in the film was equal to that of the target.

Target	Ba	Pr	La	Fe	Ni
$Ba_{1.33}Fe_{12}O_{19+y}$	1.08	⋯	⋯	12.0	⋯
$Ba_{0.93}Pr_{0.3}Fe_{11.7}Ni_{0.45}O_{19+y}$	0.71	0.30	⋯	11.7	0.38
$Ba_{0.93}La_{0.3}Fe_{11.7}Ni_{0.45}O_{19+y}$	0.64	⋯	0.30	11.7	0.37

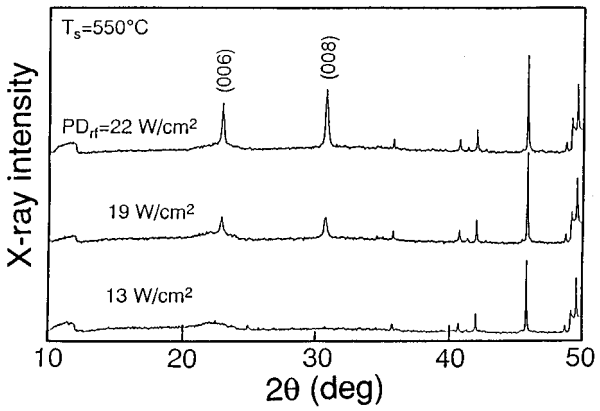

FIG. 1. Typical x-ray diffraction spectra of BaM films sputtered at various rf power densities and $T_s=550$ °C.

than that of the Ba ferrite film shown in Fig. 3(c) for comparison. The single-crystal-like diffraction spots observed at the selected area of about 400 nm in diameter suggested that crystal grains as large as 200–300 nm were present in the film.

The microstructure of the films has significant influence on the magnetic properties. Figure 5 shows the saturation magnetization (M_s), coercive force (H_c), and ratio (R_s) of remanent magnetization to M_s in $Ba_{1-x}Pr_xFe_{12-x}Ni_xO_{19}$ ($x=0.38$) films at room temperature, plotted as a function of PD_{rf}. With increasing PD_{rf}, M_s is elevated, reaching 320 emu/cc at $PD_{rf}\geqslant 15$ W/cm^2, while H_c and R_s are reduced linearly. We obtained the same M_s of 380 emu/cc as the bulk value for the nonsubstituted Ba hexaferrite films deposited at

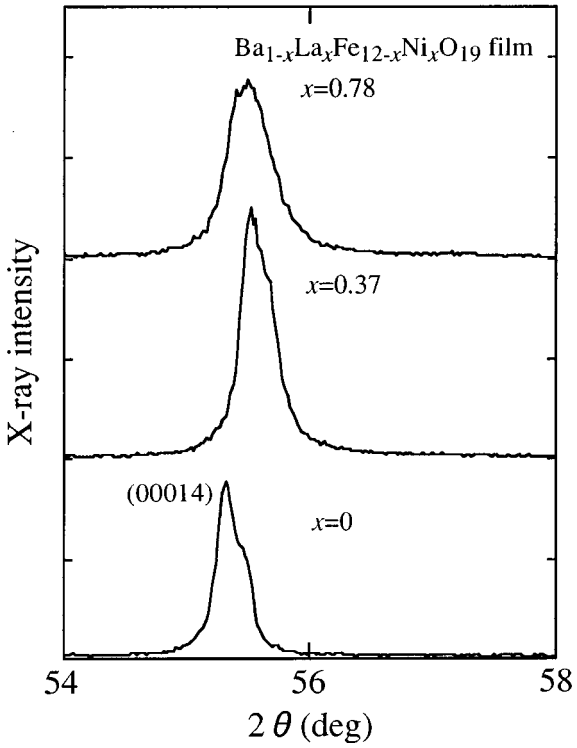

FIG. 2. X-ray diffraction spectra of the (00014) plane for films with $x=0$, 0.37, and 0.78.

Downloaded 25 Aug 2010 to 133.68.192.95. Redistribution subject to AIP license or copyright; see http://jap.aip.org/about/rights_and_permissions

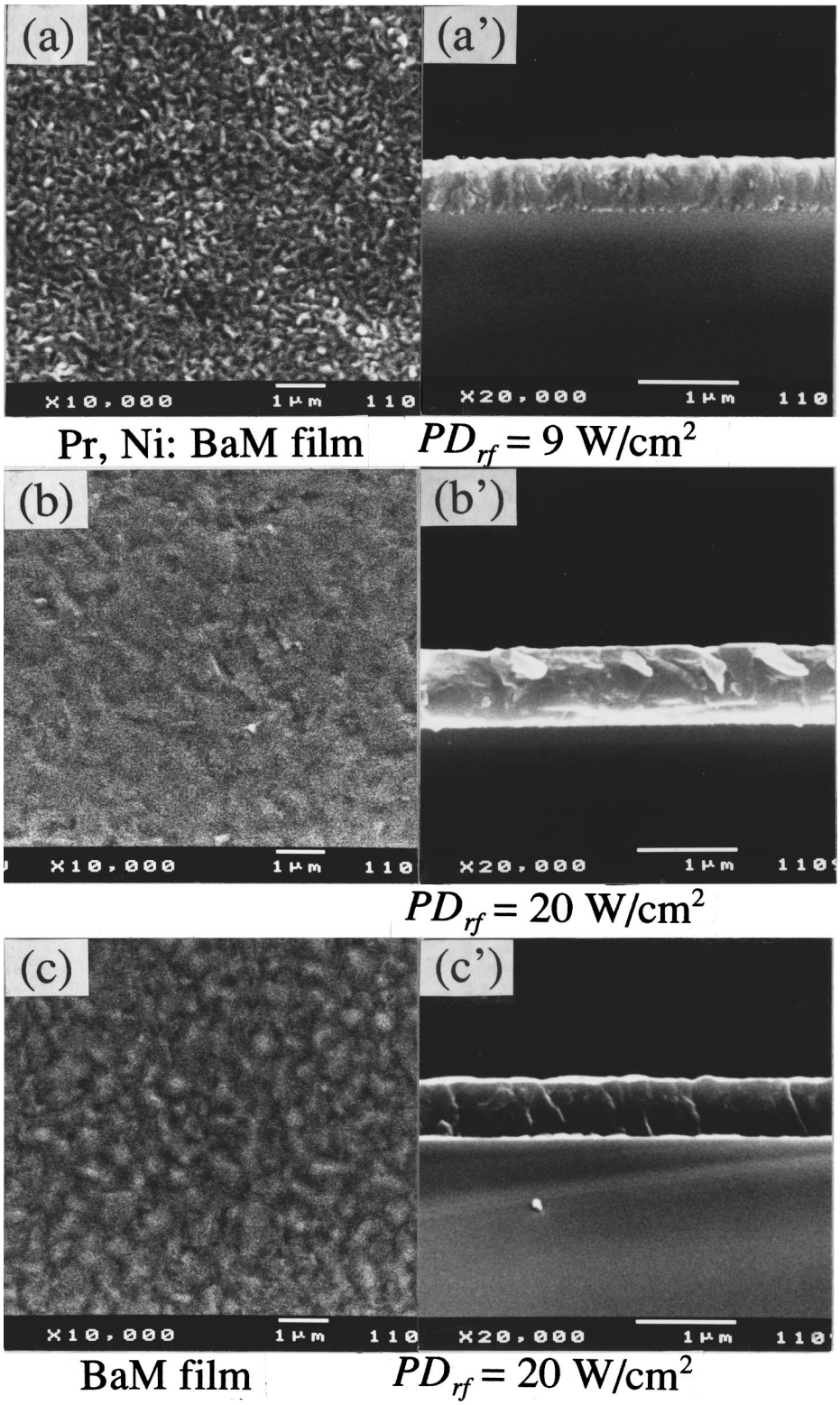

FIG. 3. Typical SEM images of the surface [(a) and (b)] and cross section [(a′) and (b′)] of $Ba_{1-x}Pr_xFe_{12-x}Ni_xO_{19}$ ($x=0.38$) films deposited at 9 and 20 W/cm^2. SEM images of the surface (c) and cross section (c′) of a BaM film deposited at 20 W/cm^2 are also shown for comparison.

$PD_{rf} \geqslant 15$ W/cm^2. The dependence of these properties on PD_{rf} is associated with the size, quality, and density of the crystallites produced in the films: In low PD_{rf}, the fine crystallites with a magnetic moment are precipitated in the nonmagnetic amorphous matrix as shown in Fig. 4(a), which results in the high H_c and low M_s of the films.

B. Magneto-optical properties

Figures 6(a) and 6(b), respectively, compare Faraday rotation spectra of the Pr–Ni substituted BaM films and the La–Ni substituted BaM films at room temperature with those of the BaM film. The spectrum for the BaM film shows some

Downloaded 25 Aug 2010 to 133.68.192.95. Redistribution subject to AIP license or copyright; see http://jap.aip.org/about/rights_and_permissions

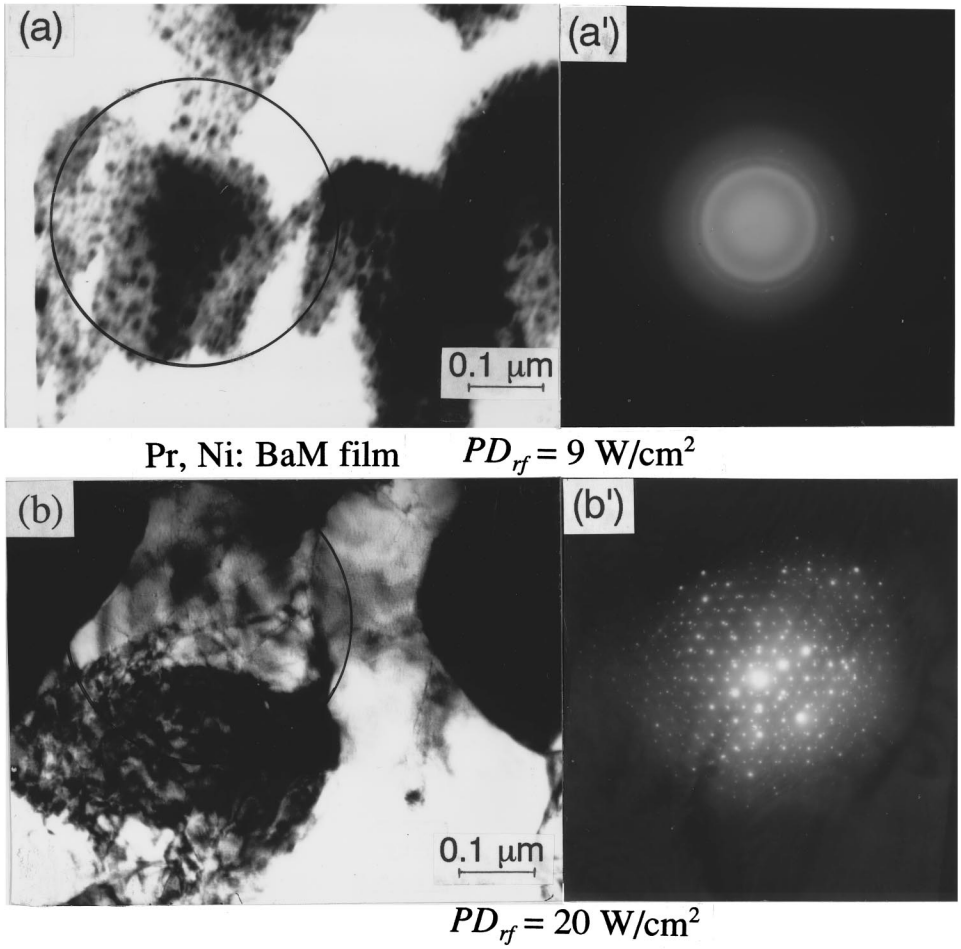

FIG. 4. Bright field TEM images [(a) and (b)] and selected area diffraction patterns [(a′) and (b′)] of $Ba_{1-x}Pr_xFe_{12-x}Ni_xO_{19}$ ($x=0.38$) films deposited at different rf power densities. The circles in the bright field images show the selected areas for electron diffraction.

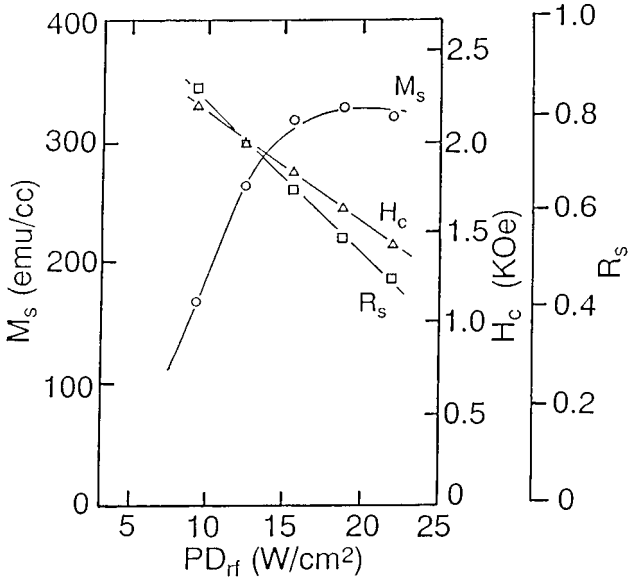

FIG. 5. Saturation magnetization M_s, coercive force H_c, and ratio R_s of remnant magnetization to M_s for $Ba_{1-x}Pr_xFe_{12-x}Ni_xO_{19}$ ($x=0.38$) films at room temperature, plotted as a function of rf power density PD_{rf}.

structure around 1.7, 2.0, 2.3, and above 2.5 eV. The structures below 2.3 eV are assigned to the crystal-field transitions of Fe^{3+} octahedrally and tetrahedrally coordinated with O^{2-} ions. This is because the observed structures have narrow spectral widths and because the optical absorption measurement showed weak peaks superimposed on a strong absorption edge at the energy positions. These observed energy positions are consistent with the previously reported positions of crystal-field transitions of the iron garnet crystal.[8] The structure above 2.5 eV is probably associated with other transitions with stronger oscillator strength located at higher energy, such as a charge transfer transition. However, details of this association are not clear at present.

As the Ni concentration increases, the Faraday rotation of the Pr–Ni substituted BaM film is reduced in the region below 2.1 eV, and especially at around 1.7 and 2.0 eV. But its negative value is enhanced in the region above 2.1 eV. The enhancement factor is as large as -1.1×10^4 deg/cm per $x=0.78$ at 2.5 eV, comparable to that of the Co^{2+} substitution reported previously (-1.3×10^4 deg/cm per Co^{2+} ion at 2.0 eV).[9] Similar spectral changes were obtained for the films substituted by the nonmagnetic La ion instead of the Pr ion, as shown in Fig. 6(b). This implies that the Pr^{3+} ion that induces a large negative rotation in the iron garnet makes no

Downloaded 25 Aug 2010 to 133.68.192.95. Redistribution subject to AIP license or copyright; see http://jap.aip.org/about/rights_and_permissions

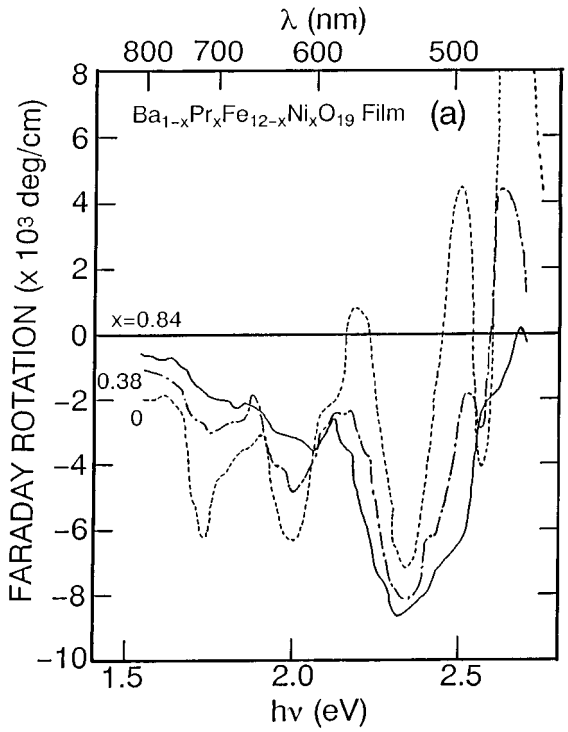

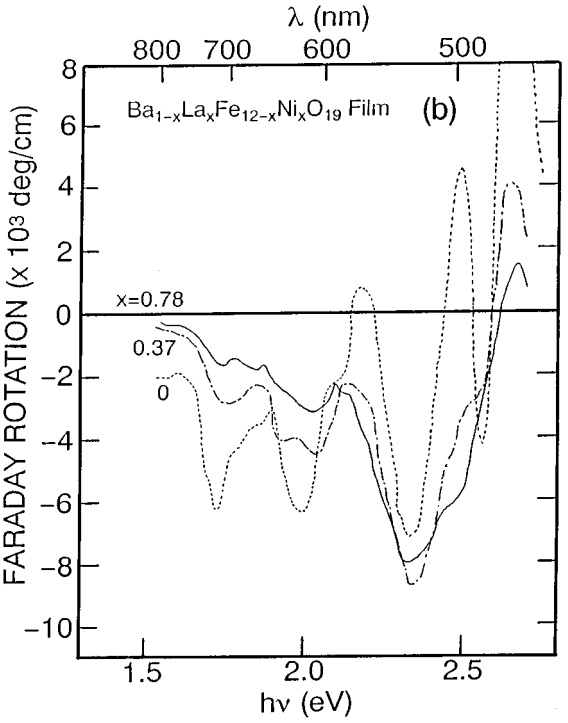

FIG. 6. Faraday rotation spectra of Pr–Ni substituted BaM films (a) and La–Ni substituted BaM films (b) at room temperature. Spectra of a BaM film are also shown for comparison.

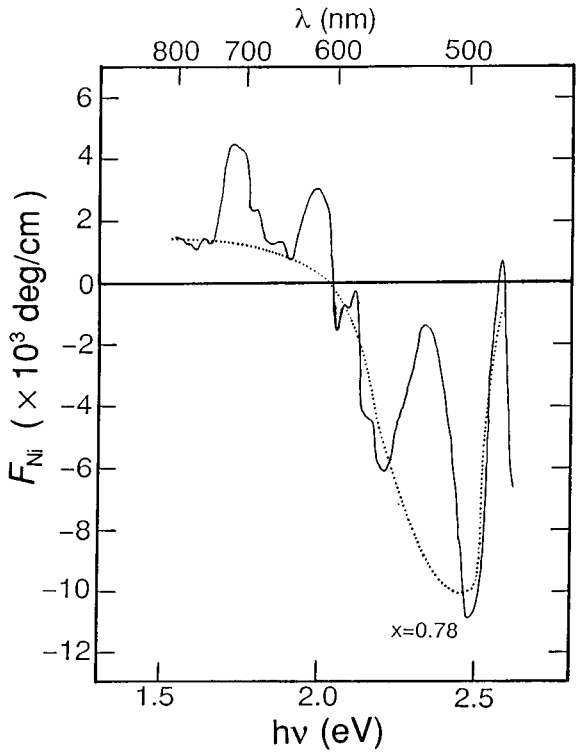

FIG. 7. Spectrum F_{Ni} (solid curve) obtained by subtracting the Faraday rotation spectrum of a nonsubstituted BaM film from that of the $Ba_{1-x}La_xFe_{12-x}Ni_xO_{19}$ ($x=0.78$) film. The dotted curve shows the intrinsic Ni^{2+} contribution to Faraday rotation schematically.

comparable contribution in the hexaferrite, at least within the photon energy range measured. Therefore, the substituted Ni^{2+} ions are primarily responsible for the observed spectral changes.

Figure 7 shows the apparent Ni^{2+} contribution obtained by subtracting the Faraday rotation spectrum of the nonsubstituted film from that of the La–Ni substituted film. It should be noted here that the subtracted values include the reduction of Faraday rotation caused by the deterioration of crystal quality. The poor crystallinity of the film induced by increasing the Ni^{2+} substitution significantly reduced the Faraday rotation, especially around the crystal-field transitions. Thus, the subtracted spectra overestimate the Ni^{2+} contribution around 1.7 and 2.0 eV, and underestimate it around 2.3 eV. The dotted curve in Fig. 7 shows the intrinsic Ni^{2+} contribution schematically. The Ni^{2+} contribution has an asymmetric spectral shape showing large negative Faraday rotation in the range of 2.1–2.6 eV and small positive rotation below 2.1 eV.

To specify the lattice sites that the Ni ions preferentially occupy in the hexaferrite, we measured x-ray photoelectron spectra of Ni $2p_{3/2}$ in the La–Ni substituted BaM film and in the Pr–Ni substituted BaM film. Figure 8 shows the results. The Ni $2p$ spectra of both films have the same binding energy (854 eV) and satellite-separation energy (7 eV) as that measured in a referent NiZn-ferrite film. This indicates that the Ni^{2+} ions preferentially occupy octahedrally coordinated sites in the hexaferrite as well as in the spinel ferrite. Pappalardo *et al.* have reported that a broad optical absorption due to a group of crystal-field transitions ${}^3A_2-{}^3_aF_1$, ${}^1_aE$ of octahedrally coordinated Ni^{2+} is observed for Ni-doped $MgAl_2O_4$ in the range of 1.9–2.5 eV.[10] We also confirmed from the diffuse reflection measurements for the ceramics of a La–Ni substituted Ba hexagallate ($Ba_{0.7}La_{0.3}Ga_{11.7}Ni_{0.3}O_{19}$) that a broad absorption induced by Ni^{2+} appears in the photon energy range of 1.6–2.4 eV.

Downloaded 25 Aug 2010 to 133.68.192.95. Redistribution subject to AIP license or copyright; see http://jap.aip.org/about/rights_and_permissions

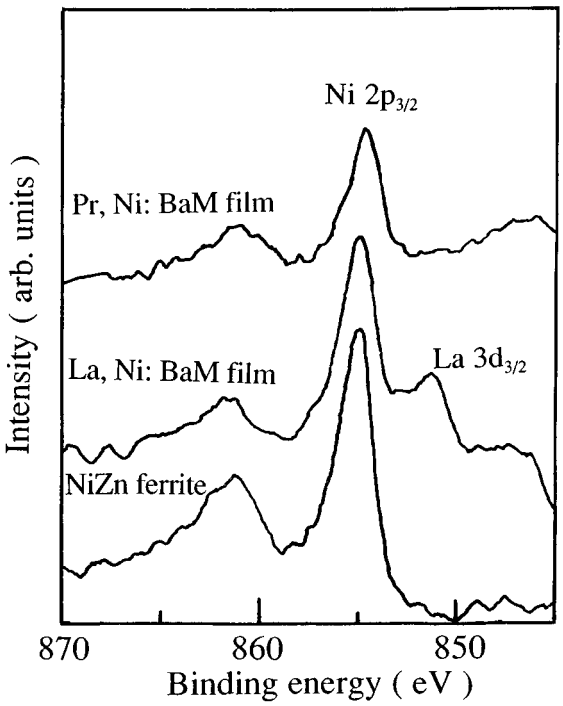

FIG. 8. X-ray photoelectron spectra for Ni $2p$ in a Pr–Ni substituted BaM film and a La–Ni substituted BaM film. The spectrum of a NiZn-ferrite film with octahedrally coordinated Ni^{2+} is also shown as a reference.

These energy ranges are in good agreement with that in which the Ni^{2+} contribution to Faraday rotation occurs. Thus, the observed spectral change of Faraday rotation by the Ni substitution is most likely attributable to the crystal-field transition of octahedrally coordinated Ni^{2+} ions.

A contribution to Faraday rotation made by other transitions lying at higher energy, such as the intraionic transition, however, cannot be ruled out. In order to conclusively determine the Ni^{2+} contribution to Faraday rotation in the hexaferrite, further complementary data, such as a Faraday ellipticity spectrum, will need to be taken in the extended photon energy range.

IV. CONCLUSIONS

We have successfully grown Pr–Ni substituted Ba hexaferrite films on GGG substrates by rf sputtering and examined the contribution of the Pr^{3+} and Ni^{2+} ions to the MO properties. The films grew with the c axis preferentially oriented normal to the film surface. The SEM and TEM observations revealed that the crystal-grain size in the films increased from several nm to about 300 nm with increasing rf power density. The films with larger grains showed higher M_s and lower H_c. The Ni substitution induced a large negative Faraday rotation in the photon energy range of 2.1–2.6 eV, while no contribution of the Pr^{3+} ion to Faraday rotation was observed. The induced spectral change is most likely ascribable to the crystal-field transitions of octahedrally coordinated Ni^{2+} ions in the 2 eV range.

[1] S. Wittekoek, T. J. A. Popma, J. M. Robertson, and P. F. Bongers, Phys. Rev. B **12**, 2777 (1975).
[2] K. Egashira, T. Manabe, and H. Katsuraki, J. Appl. Phys. **42**, 4334 (1971).
[3] S. Visnovsky, R. Krishnan, V. Prosser, S. Novak, and I. Barvik, Physica B **89**, 73 (1977).
[4] M. Gomi, K. Satoh, and M. Abe, Jpn. J. Appl. Phys., Part 2 **27**, L1536 (1988).
[5] R. K. Ahrenkiel and T. J. Coburn, IEEE Trans. Magn. **MAG-11**, 1103 (1975).
[6] M. Abe and M. Gomi, J. Appl. Phys. **53**, 8172 (1982).
[7] X. Zhang, Y. Xu, M. Duan, and M. Guillot, J. Appl. Phys. **79**, 5979 (1996).
[8] G. B. Scott, D. E. Lacklison, H. I. Ralph, and J. L. Page, Phys. Rev. B **12**, 2562 (1975).
[9] H. Nakamura, F. Ohmi, Y. Kaneko, Y. Sawada, A. Watada, and H. Machida, J. Appl. Phys. **61**, 3346 (1987).
[10] R. Pappalardo, D. L. Wood, and R. C. Linares, J. Chem. Phys. **35**, 1460 (1961).

Downloaded 25 Aug 2010 to 133.68.192.95. Redistribution subject to AIP license or copyright; see http://jap.aip.org/about/rights_and_permissions